# ARTICLES

## Thermodynamic Analysis of the Chemical Exchange of β−Phosphorylated Cyclic Nitroxides by Using Two-dimensional (Temperature versus Magnetic Field) Simulation of ESR Spectra: The Impact of Labile Solvent−Solute Interactions on Molecular Dynamics

**Antal Rockenbauer,*,† Nóra V. Nagy,† François Le Moigne,‡ Didier Gigmes,‡ and Paul Tordo‡**

*Chemical Research Center, Institute of Structural Chemistry, H-1025 Budapest, Pusztaszeri út 59, Hungary, and Laboratoire Structure et Réactivité des Especes Paramagnetiques, UMR 6517, CNRS-Universités d'Aix-Marseille I, Case 521, 13397, Marseille, Cedex 20, France*

*Received: February 27, 2006; In Final Form: May 26, 2006*

A complete thermodynamic characterization of the chair-to-chair interconversion in β-diphosphorylated piperidine-*N*-oxyl radicals was achieved by means of the analysis of temperature-dependent ESR spectra. A new two-dimensional simulation method was developed with the coordinates temperature and magnetic field, in which the entire set of spectra was simulated simultaneously by adjusting the coefficients in the power expansion, giving the temperature-dependent ESR parameters and the thermodynamic and kinetic parameters determining the site populations and exchange rates, respectively. The new method promotes elimination of the ambiguities inherent in the spectroscopic determination of thermodynamic parameters. Labile solvent−solute interactions can strongly influence the chemical exchange, producing a complex network of symmetric and asymmetric interconversions. The solvent dependence of magnetic relaxation was also analyzed.

### Introduction

The phenomenon of chemical exchange is basically related to the molecular symmetry, which can yield degenerate ground conformations. In this case, the molecule will interconvert between symmetry-related geometries, the motion of which can affect the shape and width of the spectrum lines if the rate of interconversion is in the interval $10^7-10^9$ Hz. Cyclic radicals containing five or six-membered rings are well-known examples, where the line width alternation (LWA) can be detected via ESR spectroscopy. Both the pseudorotation and the inversion process can produce interconversion, which is typically much faster for the five-membered ring than for the six-membered ring. This is why LWA can be seen with the matrix technique in the former case only at low temperature,[1] whereas in the latter case LWA appears at around room temperature.[2] The presence of a heteroatom in the ring, such as the nitrogen in cyclic nitroxyl radicals, blocks the pseudorotation and allows only oscillation between two conformers separated by a significant barrier. For the five-membered pyrrolidine (P5) ring, the ground twist conformations, i.e., $^3T_4$ and $^4T_3$, are related by the reflection $C_v$, and thus 2,5-diphosphoryl substitution retains the symmetry for the cis configuration. The large phosphorus couplings offer a good possibility for the observation of a marked LWA.[3] For the six-membered piperidine (P6) radicals, the ground chair conformers are related by the rotation $C_2$, and thus, the 2,6-diphosphoryl substituents should have trans geometry for the degeneracy to be maintained. In P5, the interconversion involves the exchange of a pseudoaxial and a pseudoequatorial phosphorus, whereas in P6, the exchange takes place between an axial and an equatorial substituent (Scheme 1). In contrast with the above cases, when P5 has a trans, or P6 a cis configuration, both substituents may occupy the preferred orientation, and thus, the ground conformation becomes nondegenerate and no exchange can occur.[3]

**SCHEME 1**

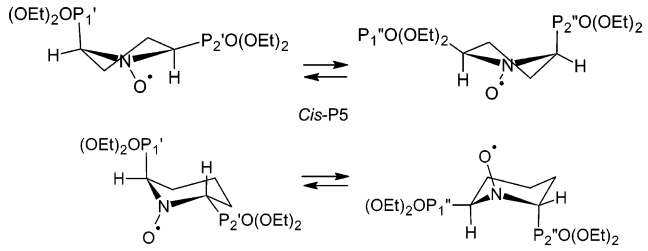


Although the molecular symmetry corresponds to exchange processes between symmetric conformers, solvent−solute interactions can reduce the actual symmetry, yielding asymmetric molecular rearrangements. The critical factor is the lifetime of the solvent−solute adducts. When the interaction is strong, the exchange does not affect the structures of the molecular associations,[4] but for labile adducts, the molecular interconversion can break the weak links between the molecules. In this case, the interconversion does not take place between two symmetry-related conformers; instead, a network of exchange processes should be considered. The best way to study this phenomenon is through the observation of coalescence, which occurs when the difference in frequency of the interconverting lines is close to equal to the rate of conformational exchange.

* Corresponding author. E-mail: rocky@chemres.hu.
† Chemical Research Center.
‡ Laboratoire Structure et Réactivité des Especes Paramagnetiques.

10.1021/jp0612331 CCC: $33.50 
Published on Web 07/14/2006

In the course of coalescence, the interconverting lines can become strongly broadened and even nonobservable at certain temperatures. The lines can completely disappear when only a single molecular interconversion takes place. If there are parallel processes, the superimposed structures of the spectra will not allow the complete extinction of all the lines. Such a situation may be expected in nonpolar aprotic solvents, where the solvate−solute interaction is weak and comparable in magnitude to the activation energy of conformational exchange.[5]

In the present study, we set out to attempt to analyze the ESR spectra of a complex exchange system, where interconversions can take place between different pairs of conformers, and for this reason a great number of independent parameters must be introduced. If the spectra are simulated separately at each temperature, the information content of the individual spectra is not sufficient for a unique solution to be obtained. This forced us to develop a new type of two-dimensional (2D) simulation method by using analogue principles applied earlier to decompose superimposed spectra recorded at different values of pH.[6] In this new method, the second coordinate is temperature and the variations in site concentration and exchange time are described by thermodynamic equations. In the course of the simulation, the ESR and thermodynamic parameters are adjusted simultaneously until the entire set of ESR spectra gives the best fit. Below, we outline the major characteristics of this method and analyze the conditions under which the information is adequate for a unique solution to be obtained with the multiparameter approach. We analyze the inherent ambiguities originating from the uncertainty principles of quantum mechanics. The analysis of the thermodynamic data permits a characterization of the different types of solvent−solute interactions affecting the molecular interconversion.

## Results and Discussion

**Line Broadening Caused by Chemical Exchange and Magnetic Relaxation.** To observe chemical exchange in the ESR spectra via LWA, we need nonzero nuclear spins in the position $\beta$ to the radical center, e.g., $^{1}$H or $^{31}$P nuclei, which possess a spin $S = {}^{1}/_{2}$. The hyperfine (*hf*) coupling of this nucleus X will depend on the dihedral angle $\Theta$ as $A_X(\Theta) = B_0 + B_2 \cos^2 \Theta$.[7] Because $\Theta$ is different for the two nuclei, the two spins will not be equivalent magnetically and the *hf* pattern of each conformation will have a double doublet structure. The line positions in this pattern can be given by combinations of the *hf* couplings:

$$-1/2(A_X(\Theta') + A_X(\Theta'')) \quad (1a)$$

$$-1/2(A_X(\Theta') - A_X(\Theta'')) \quad (1b)$$

$$1/2(A_X(\Theta') - A_X(\Theta'')) \quad (1c)$$

$$1/2(A_X(\Theta') + A_X(\Theta'')) \quad (1d)$$

respectively.

Although the interchange of $\Theta'$ and $\Theta''$ does not affect the positions of the external lines, the two central lines will be exchanged. As a consequence, the central lines can broaden, coalesce, or form a single line in the center, depending on the rate of interconversion relative to the difference of the coupling constants, $A_X(\Theta') - A_X(\Theta'')$.[8] If the exchange is slow, two separate lines may be detected in the center; when it is fast, only one line can be seen; an intermediate rate of exchange may produce coalescence, when the central lines cannot be detected at all.

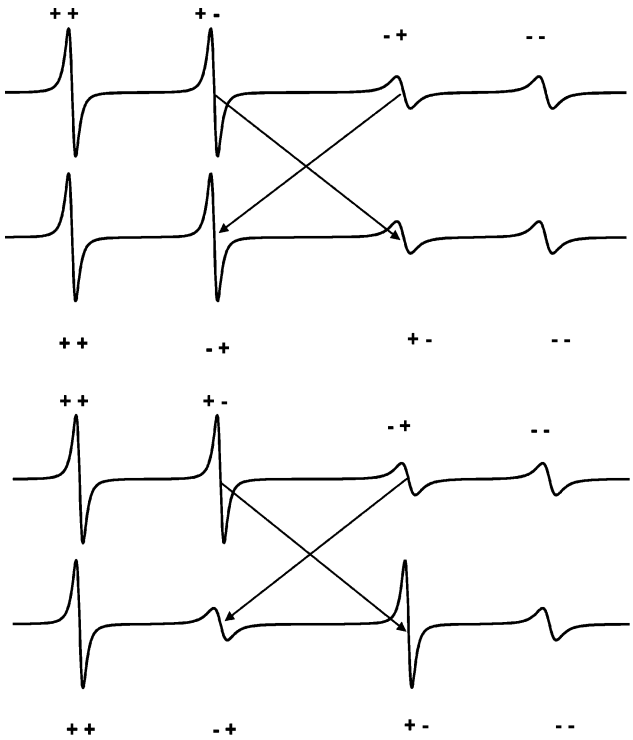


**Figure 1.** Alternative models for the phosphorus *hf* quartet on the assumption of different intrinsic line widths for the states $M_P$ and $M_P'$ denoted by the symbols + and −. (Top) Exchange of the inner lines takes place between the broad and the narrow lines. (Bottom) Exchange occurs between two broad and two narrow lines.

Besides the chemical exchange caused by intramolecular interconversion, the molecular reorientation will also affect the line width via the magnetic relaxation. In the spectra where both large nitrogen and phosphorus *hf* couplings are present, the dependences of the $M_N$ and $M_P$ magnetic quantum numbers on the line width can be given as:

$$W_{MN,MP} = \alpha + \beta M_N + \gamma M_N^2 + \beta' M_P + \gamma' M_P M_N \quad (2)$$

Although there are two phosphorus couplings, in the following, we consider only the relaxation produced by the larger coupling, because the rate of relaxation depends quadratically on the anisotropic *hf* constants.[9] In consequence of the different relaxing abilities of the two phosphorus nuclei, the line widths within the *hf* quartet are not the same, and the exchange can take place in two different ways: either between the broad and the narrow lines (top part of Figure 1) or between two broad lines and two narrow ones (bottom part of Figure 1).

In the following computations, both possibilities were tested, and it was found that the broad to sharp transitions always gave the better simulations, in accordance with expectations, because the molecular reorientations producing the relaxation are much faster than the ring inversion in either the P5 or the P6 ring.

**Principles of the 2D Simulation Program.** A complete description of the exchange network would require at least three types of exchange processes: exchange between the conformations of nonassociated radicals, that between associated radicals, and asymmetric exchange between an associated and a nonassociated radical. In principle, the system could be even more complex, because different kinds of solute−solvent interactions are possible. In practice, however, we introduce certain limitations, because a network that is extremely complex will hardly allow a unique solution to be obtained. Because the solvent−solute interactions can always reduce the actual symmetry, we

assume asymmetric interconversions, but we limit the number of exchanging pairs in the practical applications to not more than two.

Let us consider first the information balance of the ESR spectra. Although we always take the resolved or nonresolved long-range splitting into account in the spectrum fitting, for simplicity, we consider only the main lines when the information balance is analyzed. When the hyperfine pattern is built up by one $^{14}N$ and two $^{31}P$ nuclei, the number of lines is 12 for the slow and 9 for the fast exchange. In the two-site exchange model, we can determine the line positions via the g-factors, $g'$ and $g''$, and the *hf* constants, $A_{P1}'$, $A_{P2}'$, $A_{P1}''$, and $A_{P2}''$. If only one pair of exchanging conformers is present, unique parameter determination is possible. A problem is encountered, however, when we would like to include two pairs of exchanging conformers: in the fast exchange domain, a unique determination for the 12 parameters is not possible. The same problem arises in the determination of the relaxation parameters from the individual line widths.

Because the rate of interconversion, or its reciprocal, the exchange time $\tau_{exc}$, has a crucial impact on the line width, it is necessary to determine 6 parameters for one pair and 12 parameters for two pairs when the LWA is analyzed. Again, we cannot determine the complete parameter set when we are in the fast exchange domain, because of the scarcity of information.

To overcome the above difficulty, we simulate a complete set of spectra, recorded as a function of temperature. We can typically record 12−20 significantly different spectra in solvents with a low freezing point and a high boiling point. Each ESR parameter has its own temperature dependence; the variation is generally small for the g-factors and long-range *hf* couplings, intermediate for the large *hf* coupling of nitrogen and phosphorus, and rather large for the relaxation parameters. We assume, however, that for all parameters the temperature dependence is smooth enough to be described by a power expansion containing no more than four terms:

$$Q = Q_0 + Q_1(T - T_0) + Q_2(T - T_0)^2 + Q_3(T - T_0)^3 \quad (3)$$

Here, we choose $T_0 = 273$ K in the computer program. Typically, for the g-factors 2, for the large *hf* couplings 3 or occasionally 4, and for the relaxation parameters 3 or 4 coefficients should be adjusted.

The exchange time can be described either by the Arrhenius equation (eq 4), or by the Eyring equation (eq 5):

$$k = 1/\tau_{exc} = A \exp(-E_a/RT) \quad (4)$$

$$k = 1/\tau_{exc} = (k_B T/h) \exp(\Delta S^{\ddagger}/R) \exp(-\Delta H^{\ddagger}/RT) \quad (5)$$

Furthermore, the relative populations can be given by the Van t'Hoff relation (eq 6):

$$K = P'/P'' = \exp(\Delta S_R/R - \Delta H_R/RT) \quad (6)$$

In the two-pair model, the relative concentrations of solvent-associated and nonassociated radicals are also given by the Van t'Hoff relation by using the entropy $\Delta S$ and enthalpy $\Delta H$ to describe the equilibrium.

In the course of the parameter adjustment procedure, when we apply the two-pair model, we have to determine 36−40 parameters affecting the line positions, and around the same number of parameters for the line width. Because we have 12−20 independent spectra with 9−12 separate lines, the available items of information both for the line width and for the position number are around 100−200, which is amply sufficient for a unique solution to be found for the adjusted parameters. The improved information balance is a major advantage of the 2D simulation, where we do not need to determine the exchange time and the population for each individual spectrum. Instead, only four thermodynamic parameters in eqs 4−6 should be adjusted. Moreover, we do not need to adjust the individual spectroscopic parameters for each spectrum but only the respective coefficients in the power expansion.

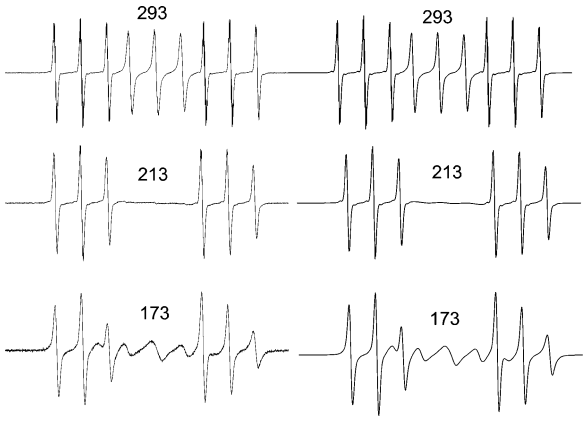


**Figure 2.** ESR spectra of trans-$\beta$-diphosphorylated pyrrolidine-*N*-oxyl radical in dichloromethane. (Left) Experimental spectra. (Right) Calculated spectra.

In the course of the spectrum simulation, we use the derivative absorption curve obtained as the solution of the extended Bloch equations.[8] For all sites, the line positions are calculated via the second-order perturbation formula of the isotropic spin Hamiltonian. The intrinsic line width data are given by eq 2, the exchange time is expressed by either eq 4 or 5, and the populations are derived by means of eq 6. The quality of fit is characterized by the sum of the square differences between the experimental and calculated points, where the summation is extended both to the field points and to the spectra recorded at different temperatures. To compare the quality of fit for different models, the noise-corrected regression coefficient is used.[6] The significance criteria are given as the change in regression corresponding to the difference in the quadratic error function, which is equal to the quadratic noise.

The most critical point in the nonlinear parameter determination is the appropriate choice of the starting values for the iteration, when the number of parameters is large. For this reason, the 2D simulation was always preceded by the simulation of the individual spectra. In this case, simplified models were applied to obtain a reliable set of parameters. When the 2D iteration was used, we combined different routes of iteration, as published earlier.[10]

**Thermodynamic Analysis of Chemical Exchange.** We carried out an analysis of the ESR spectra for P5 in pentane by the 2D simulation to compare the thermodynamic parameters with those for P6 in different solvents.

In the cases where good coalescence was found (P5 in pentane, P6 in toluene, dichloromethane (*dclm*) or diethyl ether (*dee*); see Figure 2), only one pair of interconverting conformers was assumed, whereas for P6 in *cp* or pentane, two pairs of interconverting conformers were taken into account, because no coalescence was observed in these cases (see Figure 3). The thermodynamic parameters are listed in Table 1.

The activation $E_a$ energy for P5 in pentane, obtained by the 2D simulation, is 3 kJ/mol larger than the value we reported previously,[3] when we used the classical one-by-one spectrum

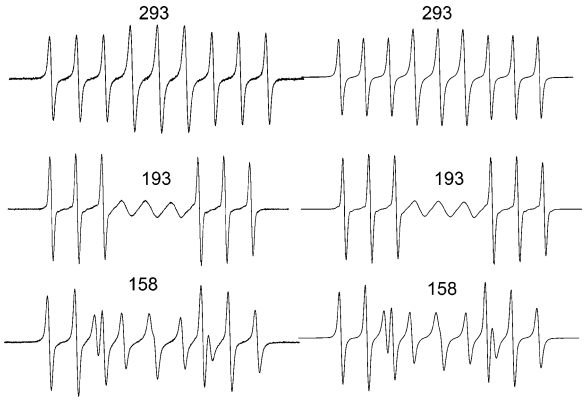


**Figure 3.** ESR spectra of trans-$\beta$-diphosphorylated pyrrolidine-*N*-oxyl radical in cyclopropane. (Left) Experimental spectra. (Right) Calculated spectra.

simulation technique. The difference is caused by the significantly reduced difference $A_{P1} - A_{P2}$ at elevated temperature, where the condition of fast exchange is valid, as compared with the case at low temperature when the exchange is slow. Although this reduction could be accounted for by the 2D simulation, the one-by-one simulation cannot offer reliable difference $A_{P1} - A_{P2}$, and thus, this value should be fixed in the calculations.

Although the molecular symmetry suggests interconversion between two mirror images (the twist conformers $^3T_4$ and $^4T_3$ for the pyrrolidine ring and two chairs for the piperidine ring), we allowed exchanges between asymmetric conformers so as to take into account the solvent−solute interactions, which could reduce the symmetry of molecular associates. In the cases when coalescence is observed, i.e., when the inner lines of the phosphorus triplet completely disappear at a certain temperature, the interconversion between two mirror conformers can give a good description of the entire set of spectra. The small values of $\Delta H_R$, $\Delta G_R$, and $\Delta S_R$ in Table 1 can be regarded as either reflecting the limit of precision in the determination of thermodynamic parameters or a consequence of the solvent−solute interactions making the interconversion slightly asymmetric.

In the weakly coordinating solvents *cp* and pentane, the spectra of piperidine derivatives demonstrate no coalescence at any temperature. In this case, the spectra were described as the superimposition of two pairs of conformers engaged in chemical exchange. The computations gave a nearly symmetric interconversion (see the first columns in Table 1 for the respective system) and a strongly asymmetric one (see the second columns in Table 1). The symmetric pair of conformers predominates at high temperature, whereas at low temperature the pairs have comparable weight or the asymmetric pair predominates. The exchange rate of the asymmetric pair is 1 or 2 orders of magnitude smaller than that of the symmetric pair, and in the temperature range where it is present in significant concentration, the exchange rate corresponds to the conditions in the slow domain, which prevents a reliable determination of the thermodynamic parameters, except for $\Delta G_R$.

The larger flexibility of the P5 ring is revealed by the smaller activation energies and the smaller difference between the enthalpies of the transition state and the ground conformers. This means that the excited conformers (more precisely, a larger domain of the pseudorotational itinerary) are more easily accessible for the P5 ring than for the P6 ring. The lower activation energy for P5 also explains why the coalescence is complete in pentane: in this case, the interconversion does not have enough energy to break the labile solvent−solute bond. The rate of exchange, however, is not necessarily higher for the P5 ring, as it is expressed by the $\Delta G^{\ddagger}$ values: the symmetric interconversion is faster for the P6 ring in weakly coordinating solvents, such as *cp* and pentane.

It is plausible to assume that symmetric interconversion takes place between two chair conformations, when the molecule is not associated with any solvent molecules, whereas the asymmetric interconversion corresponds to a molecular reorganization, when a solvent-coordinated molecule is transformed to a noncoordinated species. The activation energy of this process is higher because the solvent−solute bonding should be broken in the course of chair-to-chair interchange. On decrease of the temperature, the concentration of the asymmetric pair increases, which indicates that the formation of the solvent−solute pair is energetically favorable. On the assumption of thermal equilibrium between the solvate-associated and nonassociated molecules, the best 2D-ESR fit gave an association enthalpy of 5.1 kJ/mol in *cp* and of 3.9 kJ/mol in pentane. These values are somewhat smaller than the enthalpy difference $\Delta H^{\ddagger}$ between the symmetric and asymmetric pairs (around 8−9 kJ/mol), but the sign of the deviation is correct and more precise agreement is not expected, because the strength of the association could differ in the transition state and in the ground conformers.

The symmetric interconversion of the P6 ring differs characteristically for strongly or weakly coordinating solvents: the entropy difference $\Delta S^{\ddagger}$ is negative in the former and positive or close to zero in the latter case. This means that the presence of a weakly bonded solvent molecule in the boat transition state can efficiently hinder the chair-to-chair conversion, whereas the lack of a bonded solvent molecule can promote the interconversion. As a consequence, the rate of exchange is lower for a strongly associating solvent, which is manifested by the enhanced free energy $\Delta G^{\ddagger}$. The entropy terms seem to play a less important role for the asymmetric conversion; in this case, the rupture of solvent−solute bonding is primarily responsible for the rather slow exchange (see Table 2).

The ESR parameters are given at temperatures where the condition of slow exchange is valid and the relaxation broadening is not too strong. The 2D simulation also affords the couplings at elevated temperature, but in this domain, the precision of coupling is less good because of the fast exchange.

As concerns the ESR parameters, the most characteristic difference between the P5 and P6 rings is revealed by the phosphorus coupling with larger splitting: it is $<50$ G in the former case and $>50$ G in the latter case. This difference indicates that the phosphoryl group has a pseudoaxial orientation in the P5 ring and axial orientation in the P6 ring. The smaller couplings $A_P2'$ and $A_P1''$ do not present a characteristic difference for the pyrrolidine and piperidine radicals; it seems that the phosphorus coupling is not sensitive as to whether the orientation is pseudoequatorial or equatorial. In weakly coordinating solvents, the symmetric and asymmetric pairs of interconverting conformers can be more easily distinguished through the differences between $A_P1'$ and $A_P2''$: the difference is at most 1 G for the symmetric, but greater than 3 G for the asymmetric pair. Among the strongly associating solvents, the difference $A_P1' - A_P2''$ is small only in *dclm* (less than 1 G), where the coalescence was most perfect. On the other hand, in toluene and *dee*, where the quality of coalescence was less perfect, this difference was found to be somewhat larger (4−7 G), indicating a more complex network of interconversion, but in these cases, the signal distortion in the coalescence is not

**TABLE 1: Thermodynamic Constants of cis-$\beta$-diphosphorylated Pyrrolidine-*N*-oxyl and trans-$\beta$-Diphosphorylated-piperidine-*N*-oxyls in Different Solvents[a]**

| | P5 | P6 | | | | | | |
|---|---|---|---|---|---|---|---|---|
| | | | | | cyclopropane[b] | | pentane[c] | |
| | pentane | dichloro-methane | toluene | diethyl ether | sym. | asym. | sym. | asym. |
| $\Delta H_R$ (kJ/mol) | 0.23 | −0.11 | 0.86 | 0.21 | 0.34 | −0.21 | 0.30 | −3.46 |
| $\Delta S_R$ (J/mol K) | −0.03 | −1.13 | −2.9 | −1.34 | −0.80 | 1.01 | −1.30 | 10.16 |
| $\Delta G_R$ (kJ/mol) | 0.30 | 0.23 | 1.72 | 0.61 | 0.58 | −0.21 | 0.69 | −6.49 |
| $E_a$ (kJ/mol) | 13.44 | 15.79 | 16.61 | 15.78 | 21.09 | 28.55 | 19.53 | 28.76 |
| $\Delta H^{\ddagger}$ (kJ/mol) | 11.66 | 13.99 | 14.75 | 14.23 | 19.64 | 27.49 | 17.93 | 28.51 |
| $\Delta S^{\ddagger}$ (J/mol K) | −18.65 | −14.57 | −16.07 | −10.96 | 19.78 | 21.01 | 7.49 | 9.63 |
| $\Delta G^{\ddagger}$ (kJ/mol) | 17.22 | 18.33 | 19.54 | 17.50 | 13.75 | 21.23 | 15.70 | 25.64 |

[a] The values $\Delta G_R = \Delta H_R - \Delta S_R T$ and $\Delta G^{\ddagger} = \Delta H^{\ddagger} - \Delta S^{\ddagger} T$ are given at 298 K. The parameters $\Delta H^{\ddagger}$, $\Delta G^{\ddagger}$, and $\Delta S^{\ddagger}$ were derived via the Eyring equation, and $E_a$ was derived via the Arrhenius equation; the quantities $\Delta H_R$, $\Delta G_R$, and $\Delta S_R$ were the same in both models. [b] $\Delta H = 5.1$ kJ/mol, $\Delta S = -29.8$ J/mol K, and $\Delta G = 14.0$ kJ/mol; thermodynamic parameters $\Delta H$, $\Delta S$, $\Delta G$ give the relative concentration in the equilibrium between the symmetric (sym.) and asymmetric (asym.) pairs. [c] $\Delta H = 3.9$ kJ/mol, $\Delta S = -22.4$ J/mol K, and $\Delta G = 33.5$ kJ/mol; thermodynamic parameters $\Delta H$, $\Delta S$, $\Delta G$ give the relative concentration in the equilibrium between the symmetric (sym.) and asymmetric (asym.) pairs.

**TABLE 2: Hyperfine Couplings of cis- and trans-$\beta$-Diphosphorylated Pyrrolidine- and Piperidine-*N*-oxyls[a]**

| | P5 | P6 | | | | | | |
|---|---|---|---|---|---|---|---|---|
| | | | | | cyclopropane | | pentane | |
| | pentane | dichloro-methane | toluene | diethyl ether | sym. | asym. | sym. | asym. |
| temp/K | 163 | 173 | 183 | 163 | 148 | | 153 | |
| $A_N'$/G | 14.07 | 13.93 | 14.57 | 13.77 | 13.60 | 14.42 | 13.34 | 13.59 |
| $A_N''$/G | 14.09 | 13.82 | 13.34 | 14.04 | 14.13 | 15.79 | 14.18 | 14.96 |
| $A_P1'$/G | 47.95 | 54.33 | 57.81 | 52.18 | 53.57 | 38.16 | 53.78 | 53.38 |
| $A_P2'$/G | 25.39 | 23.96 | 22.14 | 24.29 | 23.58 | 25.67 | 23.93 | 29.16 |
| $A_P1''$/G | 23.99 | 22.86 | 24.36 | 22.09 | 24.08 | 37.29 | 23.44 | 25.03 |
| $A_P2''$/G | 48.14 | 54.00 | 50.65 | 56.35 | 54.30 | 56.15 | 54.86 | 49.74 |

[a] Long range *hf* couplings at 293 K: $A_{Me}(6) = 0.39$ G, $A_{H\gamma}(4) = 0.45$ G, $A_{H\delta}(2) = 0.30$ G.

large enough to allow a distinction between symmetric and asymmetric pairs of exchange.

**The Role of the Uncertainty Principle in the Determination of Kinetic Constants.** There is an inherent uncertainty in activation energy determinations. The uncertainty is rooted in the quantum mechanics, which poses a limit to the precision of energy measurements if the time available for the measurements is limited:

$\delta E \cdot \delta t \geq \hbar$, where $\hbar$ is the Planck constant. In spectroscopy, where we are interested in the frequency, this relation may be converted to $\delta\omega \cdot \delta t \geq 1$. Because this relation does not include the Planck constant, it extends the uncertainty to macroscopic measurements applied in any form of spectroscopy. Let us consider, for example, the solution of extended Bloch equations in magnetic spectroscopy. If the system interconverts between two states and the lifetime is shorter than the reciprocal of the separation $A' - A''$, then the line shape will approach a function with the center $P'A' + P''A''$ and the width $P'P''(A' - A'')^2\tau_{exc}$.[8] Thus, at elevated temperature, where the exchange is fast, we can determine only the average *hf* constants and we can derive information for the exchange time from the exchange broadening (see Figure 4). Although the function of the line shape explicitly includes $A'$ and $A''$, their determination becomes more and more uncertain as the exchange becomes faster, and this causes a great error when $\tau_{exc}$ is calculated. At low temperature, where the exchange time is long, the populations $P'$ and $P''$ and the *hf* couplings $A'$ and $A''$ can be determined with high precision, because the two central lines separated by $A' - A''$ can be detected, but in this case, the exchange broadening will be proportional to the inverse of $\tau_{exc}$, which is generally small relative to the relaxation. A convenient way to determine the temperature variation of $\tau_{exc}$ is to use the exchange broadening $P'P''(A' - A'')^2\tau_{exc}$ and fix the value $A' - A''$ obtained at low temperature. This method, however, may give too small a $\tau_{exc}$ value at elevated temperature, because the separation $A' - A''$ could be significantly smaller in the temperature domain of fast exchange than in the case of slow exchange, because the pseudorotation becomes more intensive. Alternatively, we can

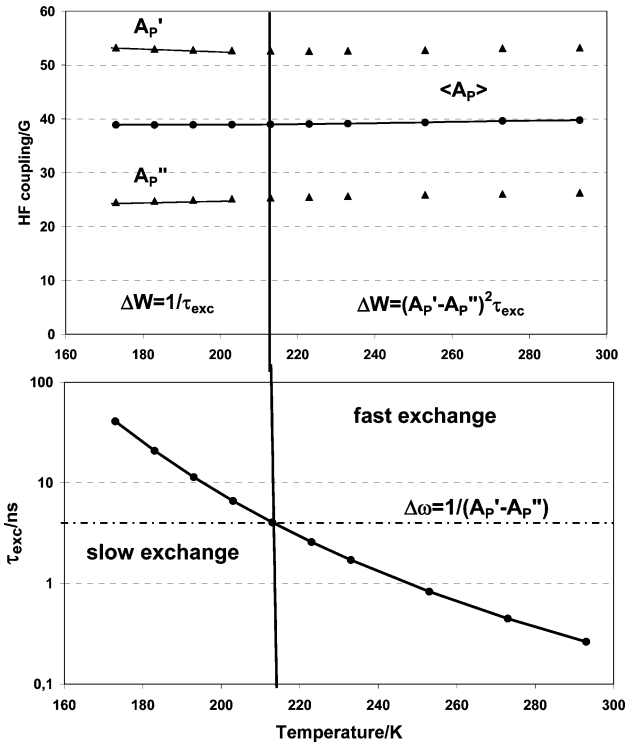


**Figure 4.** Variation of the *hf* constant (top) and exchange time (bottom) as a function of temperature. Thick vertical lines separate the slow exchange and fast exchange domains. Points connected by a solid line indicate the experimentally observed quantities. Exchange time corresponding to the coalescence is shown by the dot−dash line.

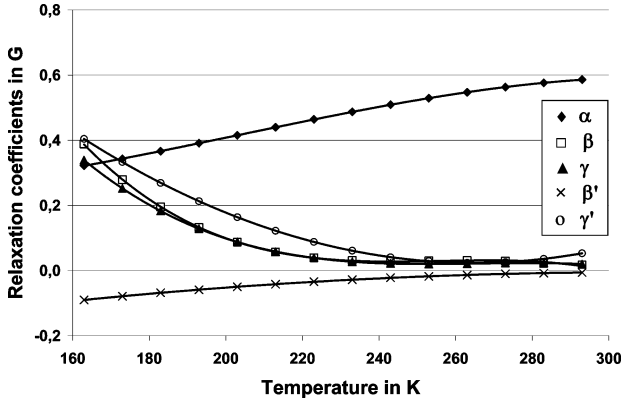


**Figure 5.** Variation of relaxation coefficients in the ESR spectra of P6 in *dee* as a function of temperature.

allow $A' - A''$ to change in the spectrum simulation, but the line narrowing observed in this case can be described by a significant decrease in $A' - A''$ instead of a shortening of the exchange time, which may lead to an overestimation of the exchange time. The 2D simulation attempts to eliminate this uncertainty by integrating the information obtained from the spectra recorded under conditions where the exchange is slow, intermediate, or fast. In this case, we obtain a more reliable $A' - A''$ value in the fast-exchange domain, and instead of the adjustment for each exchange time $\tau_{exc}$, the thermodynamic activation energy is adjusted directly in the fitting procedure.

**Solvent and Temperature Dependences of Magnetic Relaxation.** The relaxation parameters defined by eq 2 can display different temperature and solvent dependences than those for chemical exchange, because in this case the rotational tumbling of the whole molecule plays a decisive role. We found that all the parameters except α reveal the same general trend in all solvents: their absolute values diminish at elevated temperature (see Figure 5). This variation is caused by the increasing rate of rotational tumbling averaging out the anisotropic magnetic interactions.[11] The complex behavior of α is produced by two different contributions: the anisotropic magnetic interaction predominant for slow tumbling and the spin-rotational mechanism prevalent at fast tumbling. For a solvent of low viscosity, α increases throughout the entire temperature domain, in consequence of the fast molecular reorientation, whereas toluene, with a rather high viscosity, represents the opposite example, where the slow tumbling results in decreasing relaxation as the temperature increases. *Dclm*, *cp*, and pentane represent the intermediate case, when the variation of α exhibits a minimum at 203 K for *cp* and pentane and at 253 K for *dclm*.

The signs of the relaxation coefficients are positive, except for that of $\beta'$. The α and $\gamma$ should always be positive, because the anisotropic interactions involve only quadratic terms of g or the *hf* tensors.[11] The signs of the further relaxation terms also depend on the convention applied. We assigned the low-field peaks to the negative $M_N$ and $M_P$ values, and consequently, the positive $\beta$ broadens the high-field line in the nitrogen triplet, whereas for the central lines $M_N = 0$, the negative $\beta'$ sharpens the high-field line in the phosphorus doublet. The opposite signs of $\beta$ and $\beta'$ indicate that the principal direction for the largest components in the hyperfine tensors $A_N$ and $A_P$ should be close to perpendicular.

In *cp* and pentane, where the analysis of the exchange process revealed the presence of two species, the species were found to differ strongly in relaxation behavior (see Figure 6). Although the large number of relaxation parameters makes the determination less reliable in this case, it is still evident that, for the species where we observe an association between the solvent and solute molecules, the relaxation is more intensive due to the slower rotational tumbling.

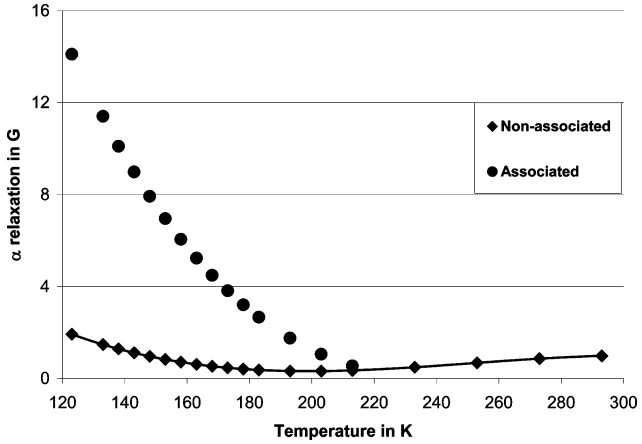


**Figure 6.** Temperature variation of relaxation parameter α in the ESR spectra of P6 in *cp*.

## Conclusions

A new 2D simulation method has been developed by using the coordinates temperature and magnetic field to determine the thermodynamic parameters of a system composed of a complex network of exchange processes. The method allows simulation of a set of spectra recorded at different temperatures by simultaneous adjustment of the spectroscopic parameters (g-factor, *hf* constants and relaxation times) and the thermodynamic parameters describing the exchange times and site populations. The ESR parameters are presumed to vary smoothly as a function of temperature and can be characterized by a power expansion containing a maximum of four terms. The 2D approach allows a unique parameter set to be obtained even when the large number of parameters would otherwise prevent the analysis if the spectra were simulated one by one. We can alternatively use the Arrhenius equation to determine the activation energy, or the Eyring equation to calculate the enthalpy and entropy. The 2D simulation can utilize the information derived from the slow, intermediate and fast exchange in an integrated way, and eliminate the uncertainty inherent in the determination of exchange time and activation energy.

The activation energy and enthalpy for the chair-to-chair inversion are larger for the trans-$\beta$- diphosphorylated piperidine ring than for the $^3T_4-{}^4T_3$ inversion in the cis-$\beta$-diphosphorylated pyrrolidine. The molecular interconversion of the piperidine ring could be a complex process due to the solvent−solute interaction, which is manifested in the ESR spectra recorded in weakly coordinating solvents not exhibiting coalescence. In strongly coordinating solvents, the interconversion takes place between nearly symmetric conformers, because the exchange process cannot break the bonding between the solvent and the solute molecules. In weakly coordinating solvents a combination of symmetric and asymmetric interconversion is observed. The asymmetric interconversion takes place between the solvent-associated and nonassociated piperidine molecules.

In the solvents *cp* and pentane, where two interconverting species are observed, the relaxation is more intensive for the solvent-associated radicals. The primary relaxation parameter, α, increases with rising temperature in *dee*, where the viscosity is small, whereas in toluene, where the viscosity makes the

rotational tumbling slow, the parameter α decreases throughout the entire temperature domain. In solvents with intermediate viscosity, α displays a minimum as a function of temperature.

## Experimental Section

ESR measurements were performed on a Bruker ESP 300 spectrometer equipped with a TM110 cavity, a Bruker variable-temperature unit ER 4111 VT and an X-band resonator (9.41 GHz). The ESR samples were deoxygenated via freeze pump thaw cycles.

The bis-phosphorylated piperidine-*N*-oxyl radicals, P6, were prepared from heptane-2,6-dione according to the procedure described for the synthesis of the corresponding bis-phosphorylated pyrrolidine-*N*-oxyl radicals.[12]

**Acknowledgment.** We thank the Hungarian Scientific Research Fund OTKA for financial support (Grant T-046953).

## References and Notes

(1) (a) Sjöqvist, L.; Lund, A.; Maruani, J. *Chem. Phys.* **1988**, *125*, 293. (b) Sjöqvist, L.; Lindgren, M.; Lund, A. *Chem. Phys. Lett.* **1989**, *156*, 323. (c)Shiotani, M.; Sjöqvist, L.; Lund, A.; Lunell, S.; Erikson, L.; Huang, M. B. *J. Phys. Chem.* **1990**, *94*, 8081.

(2) (a) Ogawa, S.; Fessenden, R. W. *J. Chem. Phys*. **1964**, *41*, 994. (b) Windle, J. J.; Kundle, J. A.; Beck, B. H. *J. Chem. Phys*. **1969**, *50*, 2630. (c) Rolfe, R. E.; Sales, K. D.; Utley, J. H. P. *J. Chem. Soc., Perkin. Trans*. 2 **1973**, 1171. (d) Gilbert, B. C.; Norman, R. O. C.; Trenwith, M. *J. Chem. Soc. Perkin Trans*. *2*, **1974**, 1033. (e) Roberts, B. P.; Steel, A. J. *J. Chem. Soc., Perkin. Trans*. 2 **1992**, 2025.

(3) Rockenbauer, A.; Gaudel-Siri, A.; Siri, D.; Berchadsky, Y.; Le Moigne, F.; Olive, G.; Tordo, P. *J. Phys. Chem. A* **2003**, *107*, 3851.

(4) Owenius, R.; Engström, M.; Lindgren, M. *J. Phys. Chem. A* **2001**, *105*, 10967.

(5) Cabani, S.; Conti, G.; Mollica, V.; Bernazzani, L. *J. Chem. Soc. Faraday Transactions* **1991**, *87*, 2433.

(6) Rockenbauer, A.; Szabó-Plánka, T.; Árkosi, Zs.; Korecz, L. *J. Am. Chem. Soc.* **2001**, *123*, 7646.

(7) (a) McConnel, H. M. *J. Chem. Phys*. **1956**, *24*, 632. (b) Heller, C.; McConnel, H. M. *J. Chem. Phys*. **1960**, *32*, 1535.

(8) Atherton, N. M. *Electron Spin Resonance, Theory and Application*; John Wiley and Sons: New York, 1973.

(9) Budil, D. E.; Lee, S.; Saxena, S.; Freed, J. H. *J. Magnetic Resonance, Ser A.* **1996**, *120*, 155.

(10) (a) Rockenbauer, A.; Korecz, L. *Applied Magn. Resonance* **1996**, *10*, 29. (b) Rockenbauer, A. *Mol. Phys. Rep.* **1999**, *26*, 117.

(11) (a) Bonora, M.; Pornsuwan, S.; Saxena, S. *J. Phys. Chem. B* **2004**, *108*, 4196−4198. (b) Kivelson, D. J. *J. Chem. Phys.* **1960**, *33*, 1094. (c) Freed, J. H.; Fraenkel, G. K. *J. Chem. Phys*. **1963**, *39*, 326. (d) Okazaki, M.; Kuwata, K. *J. Phys. Chem*. **1984**, *88*, 4181−4184.

(12) Le Moigne, F.; Tordo, P. *Acad. Sci. Paris, Chimie* **2001**, *4*, 585−590.